



Original papers

A two-layer intelligent decision-making framework for optimizing irrigation and fertilization scheduling in irrigated farmland systems

Yue Li^{a,b,c,d}, Min Hu^{a,b,c,d}, Zhijun Chen^{a,b,c,d}, Yufei Han^{a,b,c,d}, Dongyang Ren^{a,b,c,d}, Xu Xu^{a,b,c,d}, Yunwu Xiong^{a,b,c,d}, Quanzhong Huang^{a,b,c,d,*}, Guanhua Huang^{a,b,c,d,*}

^a State Key Laboratory of Efficient Utilization of Agricultural Water Resources, Beijing, China

^b Observation and Research Station for Efficient Utilization of Water Research in Hetao Irrigation District of Inner Mongolia, Ministry of Water Resources, China

^c Center for Agricultural Water Research in China, China Agricultural University, Beijing, China

^d Chinese-Israeli International Center for Research and Training in Agriculture, China Agricultural University, Beijing, China



ARTICLE INFO

Keywords:

AI Agent
Intelligent decision-making method
Irrigated farmlands
Sustainability index
Irrigation and fertilization times

ABSTRACT

Optimizing irrigation and nitrogen fertilization times (INFT) is crucial for enhancing agricultural productivity and benefits while reducing non-point source pollution and climate impacts in irrigated farmland systems. However, intelligent decision-making approaches that can efficiently and stably balance agronomic, economic, environmental, and climatic indicators to generate appropriate INFT remain limited. Here, a two-layer intelligent decision-making framework was developed based on an AI platform. In Layer 1, an agro-hydrological model (AHC) was coupled with three multi-criteria decision-making (MCDM) methods (VIKOR, TOPSIS, and AHP) to balance key indicators and generate candidate INFT solutions. In Layer 2, candidates were evaluated using a sustainability index (SUSI) based on decision indicators, including positive ones: irrigation water productivity (IWP), partial factor productivity of nitrogen (PFP_n), economic benefits (EB), and yield, and negative ones: nitrogen pollution load (NPL) and global warming potential (GWP). The framework was applied to wheat and maize farmlands in the Hetao Irrigation District of Northwest China across 48 scenarios combining irrigation and nitrogen application times with different hydrological years. Initially, candidate solutions were screened to ensure high performance in positive indicators while reducing NPL and GWP. Then, the optimal strategy was selected by maximizing SUSI across all decision indicators. Compared to local traditional practices, the optimal INFT achieved substantial improvements of 3.7–39.2% in yield, EB, IWP, and PFP_n, alongside significant reductions of 20.8–51.2% in NPL and 3.1–9.6% in GWP across wet, normal, and dry years in wheat and maize farmlands. These improvements led to significant increases in the SUSI of wheat and maize farmland systems by 28.5–106.9% relative to the local control scenarios in three hydrological years. Moreover, the AI-based decision-making framework reduced the time required for per full decision cycle to just 6–9% of that need by traditional approaches, which rely on externally linked modules. This reduction was achieved by replacing extensive manual steps, including extracting model outputs, converting data formats, calculating decision indicators, and executing MCDM procedures, with an AI platform. The two-layer intelligent decision-making framework proposed in this study offers a feasible pathway for formulating efficient and sustainable irrigation-fertilization strategies. It highlights the potential of AI platforms to enable automation and intelligent management in complex agricultural systems.

1. Introduction

Irrigation and nitrogen fertilization are key management practices for enhancing agricultural productivity and are widely used to mitigate

yield losses caused by drought and low soil fertility, especially in irrigated farmland systems (e.g., wheat and maize) (López-Bellido et al., 2005; Du et al., 2025). Although these practices have been essential for ensuring food security, unsustainable water and nitrogen management

* Corresponding author at: State Key Laboratory of Efficient Utilization of Agricultural Water Resources, Beijing, China.

E-mail address: ghuang@cau.edu.cn (G. Huang).

<https://doi.org/10.1016/j.compag.2026.111721>

Received 15 January 2026; Received in revised form 18 March 2026; Accepted 27 March 2026

Available online 2 April 2026

0168-1699/© 2026 Elsevier B.V. All rights reserved, including those for text and data mining, AI training, and similar technologies.

in recent decades has resulted in substantial environmental and economic costs. Globally, single applications with large amounts of irrigation water and nitrogen fertilizer exacerbate deep percolation and nitrate leaching, reducing irrigation water productivity (IWP) and partial factor productivity of nitrogen (PFP_n), while increasing nitrogen pollution load (NPL) and economic benefits (EB) losses in irrigated wheat and maize farmland systems (Lu et al., 2019; Bhandari et al., 2020; Li et al., 2020a). In contrast, overly frequent irrigation and fertilization not only raise labor inputs and costs, but may also aggravate greenhouse gas (GHG) emissions and global warming potential (GWP) by repeatedly altering soil moisture and nutrient dynamics (Tongwane and Moeletsi, 2018; Kamran et al., 2023). Therefore, identifying appropriate irrigation and nitrogen fertilization times (INFT) is critical for addressing these conflicts and promoting sustainable irrigated agriculture.

An efficient method is crucial for determining appropriate INFT for irrigated farmland systems. Early studies relied on field experiments to identify suitable INFT. For instance, López-Bellido et al. (2005) examined nitrogen fertilization times in irrigated wheat farmlands in Southern Spain, and Shi et al. (2018) determined the optimal irrigation stages for maize farmlands in Northwest China. However, field experiments-based approaches are often constrained by regional and climatic variability and are time-consuming and labor-intensive, limiting their broader applicability (Mon et al., 2016; Li et al., 2022). With technological advances, the agro-hydrological model-based approaches have increasingly been used to explore INFT in irrigated farmland systems (Darouich et al., 2022; Qi et al., 2024). For example, Huang et al. (2022) optimized the irrigation and nitrogen fertilization times for wheat across different hydrological years using AquaCrop model, while Wu et al. (2023) developed a framework by integrating AHC (Agro-Hydrological & chemical and Crop systems simulator) model with multi-criteria decision-making (MCDM) to improve irrigation and fertilization schedules for maize. Although these methods reduce labor and time costs, their decision-making efficiency and level of intelligence remain limited because they still require substantial manual intervention (e.g., data processing and model operation). In addition, many existing studies rely heavily on expert judgment or a single MCDM method to identify management strategies, which increases uncertainty in the outcomes.

Rapid advancements in artificial intelligence (AI) offer new opportunities to develop stable and intelligent methods for balancing productivity, environmental impacts, and economic viability in designing appropriate INFT (Li et al., 2023a; Puig et al., 2025). For instance, Du et al. (2025) developed an intelligent decision-making framework that combined the DSSAT model with machine-learning algorithms to optimize irrigation and fertilization rates and application stages for wheat. Although machine learning improved the computational efficiency in evaluating decision indicators, its autonomy and stability in generating robust optimal solutions still need to be strengthened. Recently, AI-based development platforms (e.g., COZE, Generative Pre-trained Transformer, and Hugging Face Agent) have enabled the integration of agro-hydrological models with MCDM methods, offering a potential pathway to address these challenges (Biazar et al., 2025; Shalwee et al., 2025). Within such platforms, a data management module (DMM) can be designed to extract and organize outputs from the agro-hydrological models and transfer them to a decision-indicator quantification module (DIQM), which can incorporate a comprehensive set of indicators (e.g., IWP, PFP_n, NPL, GWP, and EB). Building on these modules, a two-layer decision module (TLDM) can be developed by combining multiple MCDM methods in the first layer with a sustainability index (SUSI) of decision indicators in the second layer to rank candidate solutions and identify appropriate INFT strategies. Module-to-module data flow can further automate data transmission and execution, enable autonomous operation and improve system intelligence (Arjona et al., 2021). Moreover, a two-layer design that integrates MCDM with SUSI may help reduce uncertainty associated with reliance on a single MCDM method. However, to the best of our knowledge, integrated decision-making

frameworks that simultaneously couple agro-hydrological models, multiple MCDM methods, and SUSI within AI development platforms remain scarce. Consequently, whether such an integrated framework can consistently generate appropriate INFT for irrigated farmland systems is still unclear.

Beyond these technical limitations, most previous studies have emphasized yield and water-fertilizer productivity when optimizing INFT (Mon et al., 2016; Huang et al., 2022), while giving limited attention to the trade-offs among agricultural productivity, environmental impacts, and economic benefits. As a result, it remains unclear whether improved INFT in irrigated farmland systems can simultaneously reconcile productivity, environmental, and economic objectives, especially when INFT is generated through AI-assisted decision-making. To address these gaps, this study aims: (1) to develop a two-layer intelligent decision-making framework on the lightweight AI platform COZE by integrating agro-hydrological models, multiple MCDM methods, and SUSI evaluation; (2) to validate the framework's ability to identify optimal INFT through case studies in irrigated farmland systems; and (3) to assess whether AI-assisted INFT can jointly enhance agricultural productivity and economic benefits while reducing environmental burdens, thereby improving overall system sustainability.

2. Methodology

2.1. Two-layer intelligent decision-making framework for optimizing INFT

COZE is a next-generation, lightweight, and modular AI development platform. By integrating data management plugins and pre-configured code plugins (Sun et al., 2025), it enables users to efficiently build complex modules for data management, transmission, computation, and decision-making analysis using Python within its built-in integrated development environment. On the COZE platform (free personal version, <https://www.coze.cn>; API rate limit of 300 requests per minute), a two-layer intelligent decision-making framework was developed (Fig. 1). This framework was achieved by integrating AHC model with MCDM methods (i.e., VIKOR, AHP, and TOPSIS) and introducing SUSI evaluation for decision indicators (i.e., yield, IWP, PFP_n, NPL, GWP, and EB). First, field experiment data were used to calibrate and validate the AHC model. Scenario analysis was then performed with AHC to generate basic data on soil NO₃-N leaching, CO₂ and N₂O emissions, and grain yield under different INFT scenarios. Next, three modules were sequentially designed within the COZE platform: DMM, DIQM, and TLDM. These modules were responsible for extracting AHC outputs, calculating decision indicators, implementing the MCDM and SUSI-based two-layer decision process, and ultimately generating the optimal INFT. Within COZE, these modules were interconnected through workflows, allowing for the full automation of the process, from data extraction and decision indicator quantification to INFT decision-making analysis. This created an end-to-end intelligent framework (Fig. 1). The process begins with the input of crop type, after which all subsequent steps, data extraction, decision indicator quantification, and two-layer decision-making, are carried out without manual intervention. The detailed functional implementation of each module is presented in Sections 2.2, 2.3, and 2.4.

2.2. AHC model description and data management module

AHC is a one-dimensional agro-hydrological model developed by Xu et al. (2018), which incorporates modules that simulate key processes such as soil water movement, organic matter turnover, and crop growth. The model employs the Richards equation for simulating soil water flow, uses the convection–dispersion equation for the transport of solutes (NH₄⁺-N and NO₃-N), and applies first-order kinetics to represent the turnover of organic matter. Phenological development and biomass

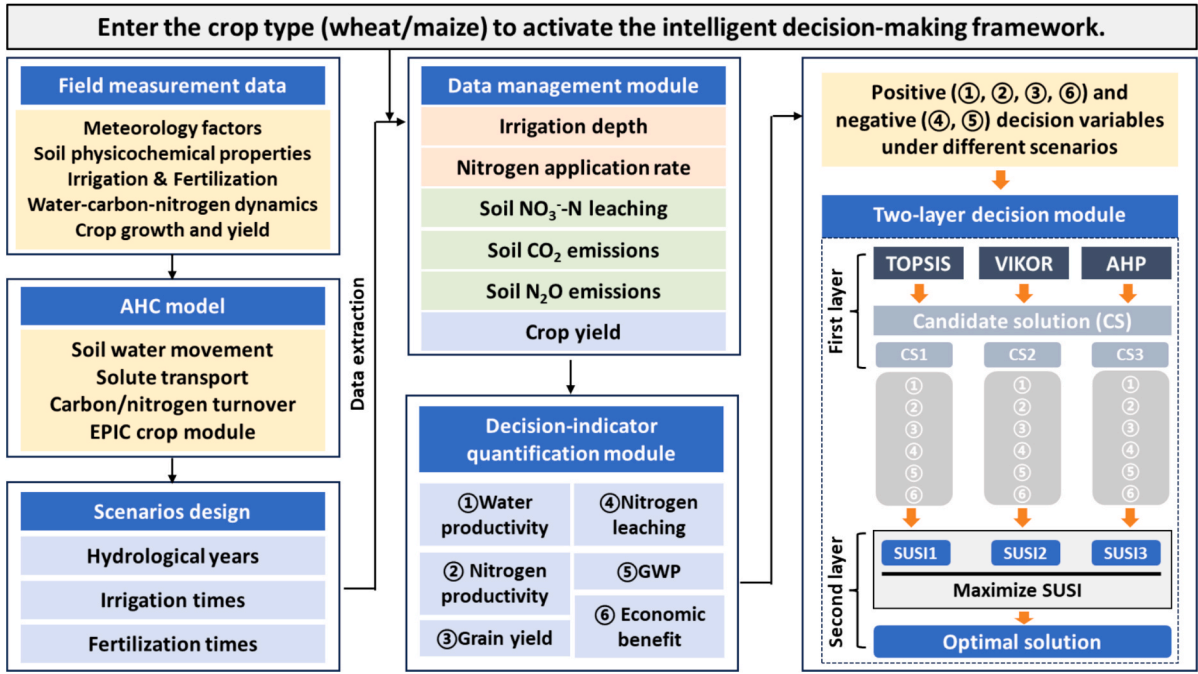


Fig. 1. Workflow of the two-layer intelligent decision-making framework.

accumulation are described using the integrated EPIC sub-model within the AHC architecture. The upper boundary condition is determined by irrigation, rainfall, and evaporation. The lower boundary is mainly related to the groundwater conditions. The governing equations for the watercarbon–nitrogen–crop growth (WCNC) processes can be found in Li et al. (2023a) and Supplementary Materials Eqs. (S1–S8).

The measured data from representative fields of the target crop are used to calibrate and validate the model parameters. To obtain the basic data required for calculating decision indicators, including IWP, PPF_n , NPL, GWP, EB, and crop yield, the calibrated AHC model is applied to conduct scenario simulations for the target crop (wheat and maize) farmlands in the study region. Scenarios with varying INFTs are designed to determine the optimal strategy for both crops (Section 3.3).

The DMM was developed using the data extraction plugin of COZE and Feishu Cloud Documentation (<https://www.feishu.cn>) to store the basic data generated from AHC simulations. The DMM retrieves the corresponding basic data, and the data extraction plugin converts these datasets into floating-point format. Upon entering the target crop type, the module is activated and automatically performs data extraction, format conversion, and data transmission to downstream modules, i.e., DIQM.

2.3. Decision indicators quantification module

The DIQM was designed to quantify the decision indicators. In the decision-making framework, the positive decision indicators include IWP, PPF_n , EB, and crop yield, while the negative decision indicators consist of NPL and GWP. The $\text{NO}_3\text{-N}$ leached from the 0–1 m soil layer can enter the groundwater, increasing the risk of non-point source pollution (Du et al., 2011; Li et al., 2022). This risk is particularly significant in regions with shallow groundwater, such as the Hetao Irrigation District of Northwest China (HIDNC), where the groundwater depth fluctuates between 1 and 2.7 m (Li et al., 2022). Therefore, the simulated $\text{NO}_3\text{-N}$ leached from the 0–1 m soil layer by the AHC model is used to estimate NPL to groundwater. Additionally, crop yield is directly simulated by the AHC model.

The IWP and PPF_n are calculated as follows:

$$IWP = 0.1 \times \frac{Y_{crop}}{I_{depth}} \quad (1)$$

$$PPF_n = \frac{Y_{crop}}{N_{rate}} \quad (2)$$

where IWP is the irrigation water productivity, kg m^{-3} ; PPF_n is the partial factor productivity of nitrogen, kg kg^{-1} ; Y_{crop} is the crop grain yield, kg ha^{-1} ; I_{depth} is the irrigation depth, mm; N_{rate} is the nitrogen application rate, kg ha^{-1} ; 0.1 is the unit transform coefficients.

The GWP is calculated as follows (IPCC, 2021; He et al., 2024):

$$GWP = \frac{C_{CO_2} + 273 \times C_{N_2O}}{1000} \quad (3)$$

where GWP denotes the global warming potential, $\text{t CO}_2\text{-eq ha}^{-1}$; C_{CO_2} is the cumulative soil CO_2 emissions during the crop growing season, kg ha^{-1} ; C_{N_2O} is the cumulative soil N_2O emissions during the crop growing season, kg ha^{-1} ; The 273 is the GWP values for N_2O to CO_2 over a 100-year time horizon (IPCC, 2021; He et al., 2024). 1000 is the unit transform coefficients.

The EB is calculated as follows (Li et al., 2020; 2022):

$$EB = p_1 \cdot Y_{crop} - p_2 \cdot I_{amount} - p_3 \cdot F_{rate} - C_{other} \quad (4)$$

where p_1 and p_3 are the crop grain and fertilizers prices, respectively, CNY kg^{-1} ; p_2 is the irrigated water price, CNY m^{-3} ; I_{amount} is the irrigation amount, $\text{m}^3 \text{ha}^{-1}$; F_{rate} is the application rate of fertilizers, kg ha^{-1} ; C_{other} is the other cost caused by seed, pesticide, plowing, sowing, harvesting, and labor for field management, CNY ha^{-1} . The values for p_1 , p_2 , p_3 , and C_{other} in maize and wheat fields are provided in our previous studies Li et al. (2020; 2022).

2.4. Two-layer decision module

The TLDM was constructed by integrating three MCDM methods (VIKOR, TOPSIS, and AHP) along with the SUSI of decision indicators [IWP, PPF_n , EB, and yield (positive decision indicators); NPL and GWP (negative decision indicators)]. In the first layer, three MCDM methods are applied to balance positive and negative decision indicators across

different INFT scenarios. Each method employs a distinct internal mechanism to identify a compromise solution that optimally balances the conflicts between positive and negative decision indicators: (1) VIKOR minimizes individual regret while maximizing group utility (Opricovic and Tzeng, 2004); (2) TOPSIS identifies the solution closest to the ideal solution and farthest from the negative-ideal solution (Opricovic and Tzeng, 2004); and (3) AHP derives a priority ranking through pairwise comparisons (Lukinskiy et al., 2025). Before performing the decision-making analysis, all negative indicators are positively transformed. Subsequently, at the first decision-making level, three preliminary candidate solutions are generated based on the principle of maximizing positive indicators while minimizing negative ones. The corresponding calculation equations for VIKOR, TOPSIS, and AHP are provided in Eqs. (5)-(13).

In the second layer, the SUSI of the decision indicators for the three preliminary candidate solutions generated by VIKOR, TOPSIS, and AHP is calculated using Eq. (14). The candidate solution with the highest SUSI value is then selected as the final optimal solution. The two-layer decision-making approach aims to mitigate uncertainties inherent in relying on any single MCDM method, while identifying a synergistic and sustainable solution (i.e., INFT) that optimally balances farmland productivity, environmental impacts, and economic benefits.

The VIKOR model can be described as follows (Opricovic and Tzeng, 2004):

$$Q_i = \nu \frac{(S_i - S^*)}{(S^- - S^*)} + (1 - \nu) \frac{(R_i - R^*)}{(R^- - R^*)} \tag{5}$$

$$S_i = \sum_{j=1}^n \omega_j \frac{(f_j^+ - f_{ij})}{f_j^+ - f_j^-} \tag{6}$$

$$R_i = \max_{1 \leq j \leq n} \left\{ \frac{\omega_j (f_j^+ - f_{ij})}{f_j^+ - f_j^-} \right\} \tag{7}$$

where Q_i represents the benefit ratio associated with the i -th scenario (the lowest Q denotes the optimal option); ν represents the decision-making coefficient; S_i and R_i represent the group utility and individual regret associated with the i -th scenario, respectively; ω_j is the weight of the j -th indicator. Among these, S^* and S^- represent the minimum and maximum values of S_i , while R^* and R^- represent the extreme values of R_i respectively.

The TOPSIS model can be described as follows (Opricovic and Tzeng, 2004):

$$E_i = \frac{D_i^-}{D_i^+ + D_i^-} \tag{8}$$

$$D_i^+ = \sqrt{\sum_{j=1}^n (\omega_j \cdot r_{ij} - \max(\omega_j \cdot r_{ij}))^2} \tag{9}$$

$$D_i^- = \sqrt{\sum_{j=1}^n (\omega_j \cdot r_{ij} - \min(\omega_j \cdot r_{ij}))^2} \tag{10}$$

$$r_{ij} = \frac{x_{ij}}{\sqrt{\sum_{i=1}^m x_{ij}^2}} \tag{11}$$

where E_i is the score value of the i -th scenario, with the highest value corresponding to the best scenario; D_i^- is the distance between the i -th scenario and the ideal scenario; D_i^+ is the distance between the i -th scenario and the worst scenario; ω_j is the weight of the j -th indicator; r_{ij} is the normalized value of the j -th indicator for the i -th scenario; x_{ij} is the original value of the j -th indicator for the i -th scenario.

The calculation equations for the AHP model are as follows (Lukinskiy et al., 2025):

$$CR = \frac{\lambda_{max} - n}{RI(n - 1)} \tag{12}$$

$$S_i = \sum_{j=1}^n \omega_j \cdot x_{ij} \tag{13}$$

where CR is the consistency ratio, and when $CR < 0.1$, the consistency of the decision matrix is acceptable; λ_{max} is the maximum eigenvalue of the decision matrix; RI is the random consistency index; S_i is the score value of the i -th scenario, with the highest value corresponding to the best scenario; n is the number of preset scenarios; ω_j is the weight of the j -th indicator; x_{ij} is the original value of the j -th indicator for the i -th scenario.

The SUSI for all positive and negative indicators is calculated as follows:

$$SUSI = \frac{\sum_{j=1}^n \omega_j \cdot PI_j}{\sum_{j=1}^n \omega_j \cdot NI_j} \tag{14}$$

where $SUSI$ denotes the sustainability index; PI_j is the j -th positive indicator, including irrigation water productivity, partial factor productivity of nitrogen, crop yield, and economic benefit; NI_j is the j -th negative indicator, including global warming potential and nitrogen pollution load. In this study, in order to eliminate the influence of different units among decision-making indicators, the SUSI were calculated based on standardized data.

The CRITIC method was employed to assign weights for all decision indicators in Eqs. (5)-(14) (Diakoulaki et al., 1995):

$$\omega_j = \frac{\sigma_j \sum_{k=1}^n (1 - r_{jk})}{\sum_{j=1}^n \sigma_j \sum_{k=1}^n (1 - r_{jk})} \tag{15}$$

where r_{jk} is the linear correlation coefficient, which represents the discordance of the j -th indicator and k -th indicator, and σ_j is the standard deviation, which quantifies the contrast intensity of the j -th indicator.

3. Application of two-layer intelligent decision-making framework

3.1. Study site

The HIDNC is a typical irrigated agricultural region located in the Inner Mongolia Autonomous Region of China (41°09'N, 107°39'E), covering a total area of 11626 km². The region experiences an average annual precipitation of approximately 140 mm, cumulative annual potential evaporation of 2240 mm, and average annual temperature of 7 °C, respectively. The annual groundwater depth fluctuates between 1 and 2.7 m (Li et al., 2022). The predominant soil textures include loam, silt loam, and sandy loam. Wheat and maize are the primary food crops cultivated in the HIDNC. From 2000 and 2021, the planting areas of wheat and maize ranged 300 to 3733 km² and from 902 to 4305 km², respectively (Li et al., 2025). Over the years, inappropriate irrigation and nitrogen application management have caused severe significant challenges in the region, including substantial water percolation, NO₃-N leaching, GHG emissions, and low IWP, PFP_n, and EB in wheat and maize farmlands (Du et al., 2011; Li et al., 2020b). Thus, wheat and maize farmlands in the HIDNC were selected as representative case studies to evaluate the performance of the two-layer intelligent decision-making framework in generating appropriate INFT, with the goal of balancing productivity, environmental impacts, and economic benefits in irrigated farmland systems.

3.2. Field data collection, model setup, calibration, and validation

Two field experiments were conducted at the Hetao Experimental Station in the HIDNC. In the first experiment, maize was cultivated in the test field during the 2017–2018 period, with five different combinations of irrigation and nitrogen application (Table S1). Irrigation depths ranged from 170 to 450 mm, and nitrogen application rates varied between 150 and 350 kg ha⁻¹. In the second experiment, wheat was planned as the test crop from 2019 to 2020. Six treatments with different irrigation and nitrogen application treatments were implemented (Table S2). For these treatments, irrigation depths ranged from 180 to 450 mm, and nitrogen application rates ranged from 170 to 340 kg ha⁻¹. In both maize and wheat experiments, data were collected on soil water, NH₄⁺-N and NO₃⁻-N contents, soil CO₂ and N₂O emissions, soil NO₃⁻-N leaching, crop height, leaf area index, dry biomass, and grain yield. Detailed information on experimental design, field management practices, sample collection, and analytical methods is provided in Li et al. (2020a) for the maize and in Li et al. (2022) for the wheat. Tables S1 and S2 can be found in the Supplementary Materials.

The steps for creating AHC simulation case in wheat and maize fields of the HIDNC as follow: the soil water and solute dynamics were simulated across a 300 cm deep vertical profile, discretized at 1 cm intervals into 301 nodes. These nodes were subsequently aggregated into 4–6 layers according to the soil texture characteristics of the test fields. The simulation period spanned from sowing to harvest of the target crops in the study region. Daily fluxes of irrigation, precipitation, and evaporation defined the upper boundary condition for soil water flow, whereas daily groundwater depth were used to set the lower boundary condition. For soil solute transport, the fluxes of solute concentrations (NH₄⁺-N and NO₃⁻-N) resulting from precipitation, irrigation, and groundwater were applied to define the upper and lower boundary conditions. Initial conditions were set according to the measured values of soil water and nitrogen content.

For two field experiments, data from the first year across all treatments were used to calibrate the parameters of the AHC model, including those related to soil hydraulics, water stress, organic matter dynamics, and crop growth (Table S3–S6). Data from the second year were then used for model validation. A parameter adjustment approach was adopted, refining the values until the AHC model accurately captured the WCNC processes under varying irrigation and nitrogen application treatments (Figs. S1–S6 and Table S7 for wheat farmlands, and Figs. S7–S10 and Table S8 for maize farmlands). The important parameters with high sensitivity and their calibrated values are shown in Table 1. Further detailed information about the calibration and

validation of AHC are available in Li et al. (2023a). Figs. S1–S10 and Table S1–S8 can be found in the Supplementary Materials.

3.3. Scenario design

To obtain the basic data (soil NO₃⁻-N leaching, CO₂ and N₂O emissions, and grain yield) required for decision-making, scenario simulations were conducted using the calibrated AHC model. Based on field surveys and relevant studies in the HIDNC (Dong et al., 2011; Peng et al., 2019; Li et al., 2020a; Li et al., 2022; Zhang et al., 2022), wheat was typically irrigated 2–5 times and nitrogen fertilized (including basal fertilizer) 3–6 times during its growing season, while maize was irrigated 3–6 times and nitrogen fertilized (including basal fertilizer) 3–6 times. For each crop, the times of irrigation and fertilization were fully randomly combined across three hydrological years (wet, normal, and dry), resulting in a total of 48 scenarios (Tables 2 and 3). Among these scenarios for wheat and maize, the combinations of three irrigations and three nitrogen applications (I3N3) correspond to the local traditional practices, which were used as the control scenarios. The total irrigation depth and total nitrogen application rate during the crop growing season were kept constant across different irrigation and fertilization times. The optimal total irrigation depths and total nitrogen application rates for different hydrological years were adopted from previous research in the HIDNC. For wheat, suitable irrigation depths were 210 mm in wet years, 240 mm in normal years, and 300 mm in dry years (Li et al., 2022; Li et al., 2023). For maize, the corresponding values were 270 mm, 300 mm, and 330 mm, respectively (Li et al., 2022). For all irrigation scenarios, the irrigation amount was evenly distributed across each stage in both wheat and maize farmlands (Tables 2 and 3). The suitable nitrogen application rate for both crops was 250 kg ha⁻¹, regardless of the hydrological year. In the study region, 50 kg ha⁻¹ of nitrogen fertilizer was applied as basal fertilizer during the seeding stage in wheat farmlands, and the remaining nitrogen was evenly distributed across the subsequent designed fertilization stages (Table 2) (Li et al., 2022). In maize farmlands, 75 kg ha⁻¹ of nitrogen fertilizer was applied as basal fertilizer during the seeding stage, and the remaining nitrogen was evenly distributed across the subsequent designed fertilization stages (Table 3) (Zhang et al., 2022). Specific dates for irrigation and nitrogen fertilization were determined based on local farming practices. Detailed information on scenario design is provided in Tables 2 and 3.

3.4. Performance comparison

Integrating agro-hydrological models with MCDM methods has

Table 1
Important parameters with high sensitivity and their calibrated values for AHC model.

Processes	Parameters	Descriptions	Calibrated values		Notes
			Wheat fields	Maize fields	
Soil water flow	θ_{s1}	Saturated water content (cm ³ cm ⁻³)	0.42	0.41	Numerical subscripts 1, 2, 3, and 4 denote the 0–25, 25–50, 50–70, and 70–100 cm soil layers, respectively.
	θ_{s2}		0.43	0.41	
	θ_{s3}		0.49	0.40	
	K_{s1}	Saturated hydraulic conductivity (cm d ⁻¹)	25	20	
	K_{s2}		15	15	
Soil solute transport	K_{s3}	10	15		
	L_{a3}	Dispersion length of NH ₄ ⁺ -N (cm)	21	20	
	L_{a4}		15	15	
Carbon/Nitrogen (C/N) turnover	L_{b3}	Dispersion length of NO ₃ ⁻ -N (cm)	15	18	Numerical subscripts 1 and 2 denote the pool with slow and fast turnover rate, respectively.
	r_1	C/N ratio in fresh organic matter pool	15	16	
	r_2		12	10	
	k_1	Decomposition rate coefficient in fresh organic matter pool	0.00012	0.00013	
	k_2		0.00035	0.00032	
Crop growth	$TOTP$	Optimal temperature for plant growth (°C)	15.5	22	
	LAI_{max}	Potential maximum leaf area index	6	7	
	THU	Total heat units required for plant maturity	2200	2700	

Table 2
Detailed scenario design for wheat farmlands in HIDNC.

Field practices	Times	Wheat growth stages					Labels	Hydrological years
		Seeding	Tillering	Jointing	Heading	Filling		
Irrigation	2		✓		✓		I2	Wet year (H1)
	3		✓	✓	✓		I3	Normal year (H2)
	4		✓	✓	✓	✓	I4	Dry year (H3)
Nitrogen fertilization	5	✓	✓	✓	✓	✓	I5	
	3	✓	✓	✓	✓		N3	
	4	✓	✓	✓	✓		N4	
	5	✓	✓	✓	✓		N5	
	6	✓	✓	✓	✓	✓	N6	

Note: scenarios = $I_i \times N_j \times H_n$ ($i = 2, 3, 4, 5$; $j = 3, 4, 5, 6$; $n = 1, 2, 3$).

Table 3
Detailed scenario design for maize farmlands in HIDNC.

Field practices	Times	Maize growth stages					Labels	Hydrological years
		Seeding	V12	Tasseling	Silking	Filling		
Irrigation	3		✓	✓		✓	I3	Wet year (H1)
	4		✓	✓	✓	✓	I4	Normal year (H2)
	5	✓	✓	✓	✓	✓	I5	Dry year (H3)
Nitrogen fertilization	6	✓	✓	✓	✓	✓	I6	
	3	✓	✓	✓	✓		N3	
	4	✓	✓	✓	✓		N4	
	5	✓	✓	✓	✓		N5	
	6	✓	✓	✓	✓	✓	N6	

Note: scenarios = $I_i \times N_j \times H_n$ ($i = 3, 4, 5, 6$; $j = 3, 4, 5, 6$; $n = 1, 2, 3$).

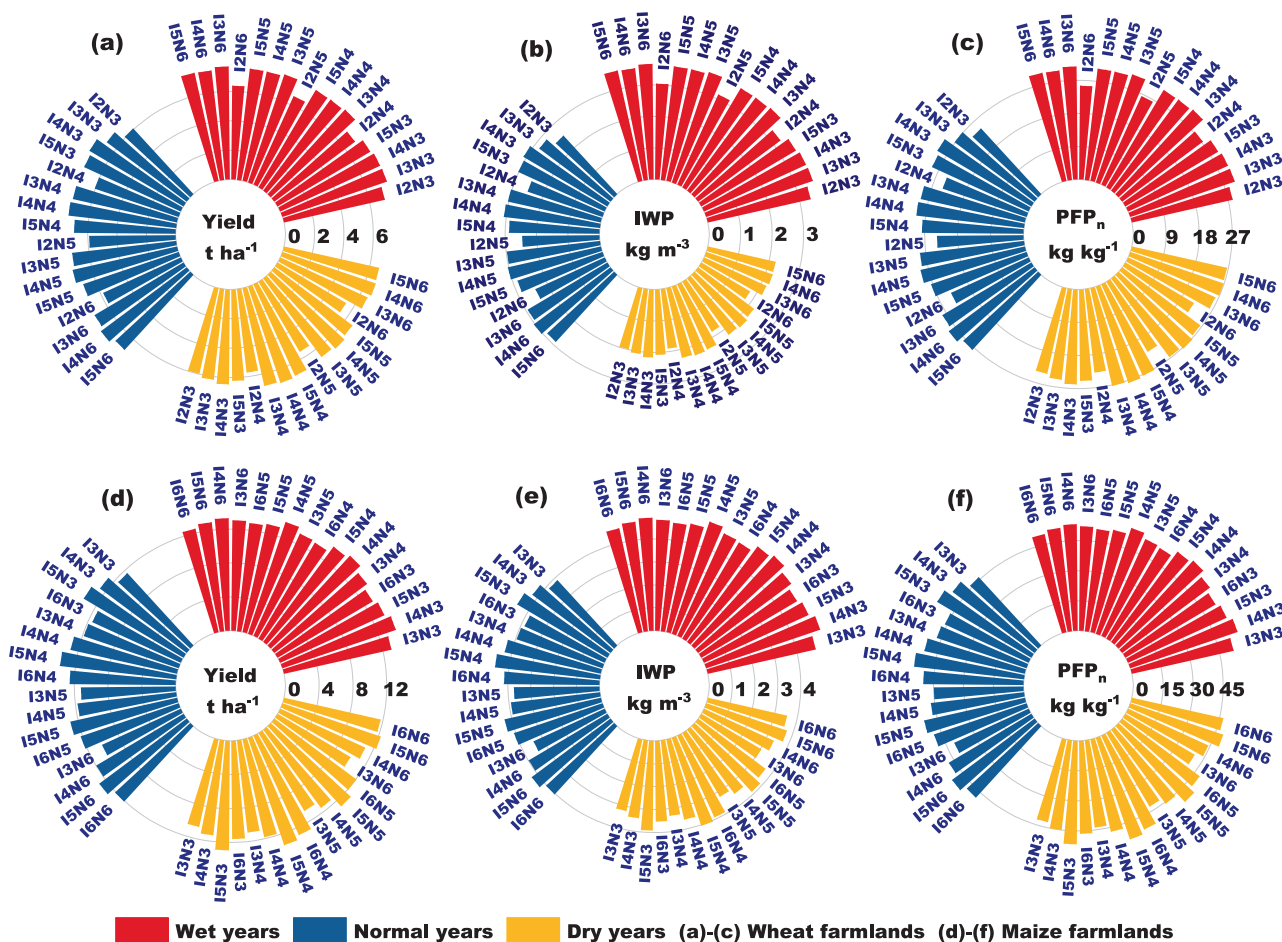


Fig. 2. Crop yield, IWP, and PFP_n across irrigation and nitrogen fertilization times scenarios for wheat and maize in wet, normal, and dry years. Note: IWP and PFP_n denote the irrigation water productivity and partial factor productivity of nitrogen, respectively.

rapidly emerged as a promising approach for optimizing agricultural management practices. This combined methodology serves as the baseline control in the present study to evaluate the advantages of the proposed intelligent decision-making framework. Specifically, Control 1 refers to the AHC model + VIKOR framework developed by Wu et al. (2023), which balances crop yield, IWP, and soil salinity to determine irrigation and fertilization strategies for maize farmlands. Control 2 corresponds to the AHC model + VIKOR framework established by Li et al. (2023a), which integrates crop yield, PFP_n, IWP, and multiple ecosystem service values to formulate irrigation and fertilization strategies for wheat farmlands. To assess the effectiveness of the proposed framework, this study compares its performance against the two controls across several key dimensions: model operation/activation, extraction of model outputs, data format conversion, calculation of decision indicators, execution of MCDM procedures, and the time required per decision cycle.

4. Results and discussion

4.1. Responses of agricultural productivity-environmental-economic indicators to various INFT

Crop yield exhibited a nonlinear response to irrigation times across wet, normal, and dry years for both wheat and maize farmlands (Fig. 2a, d). As the number of irrigation events increased, i.e., from 2 to 5 times for wheat and from 3 to 6 times for maize, crop yield increased first and then decreased. Specifically, for wheat, the highest yield was achieved

under three irrigation events in wet years and four events in normal and dry years. For maize, the optimal times that resulted in the highest yield were four irrigations in wet years and five irrigations in normal and dry years. The responses of IWP, PFP_n, and EB to irrigation times aligned with those of yield across all hydrological years and crop types (Fig. 2b, c, e, f and Fig. 3c, f). In contrast, the negative indicators displayed opposing trends, i.e., NPL decreased significantly as irrigation events increased (Fig. 3a, d), while GWP showed an upward trend (Fig. 3b, e).

Increasing nitrogen application times had a negative impact on crop yield, IWP, PFP_n, and EB for both crops across all hydrological years (Fig. 2 and Fig. 3c, f). Even so, appropriately increasing nitrogen application times helped reduce GWP without increasing NPL (Fig. 3a, b, d, e). The synergistic response of these productivity, environmental, and economic indicators to varying INFT demonstrates the feasibility of maintaining high crop yield, IWP, and PFP_n, while simultaneously keeping low GWP and NPL through the optimization of INFT.

4.2. Decision-making of optimal INFT for wheat and maize farmlands

A single MCDM method introduces considerable uncertainty into the decision-making solutions (Ye et al., 2025). At the first decision-making level, VIKOR identified I2N6 as the candidate INFT for wheat farmlands in all three hydrological years. Using AHP, the corresponding candidate solutions were I3N4, I4N4, and I3N3 for wet, normal, and dry years, respectively, whereas TOPSIS selected I5N3, I5N3, and I4N4 under the same conditions (Fig. 4). For maize farmlands, the candidate INFT selected by VIKOR was I3N6 in all three hydrological years. AHP

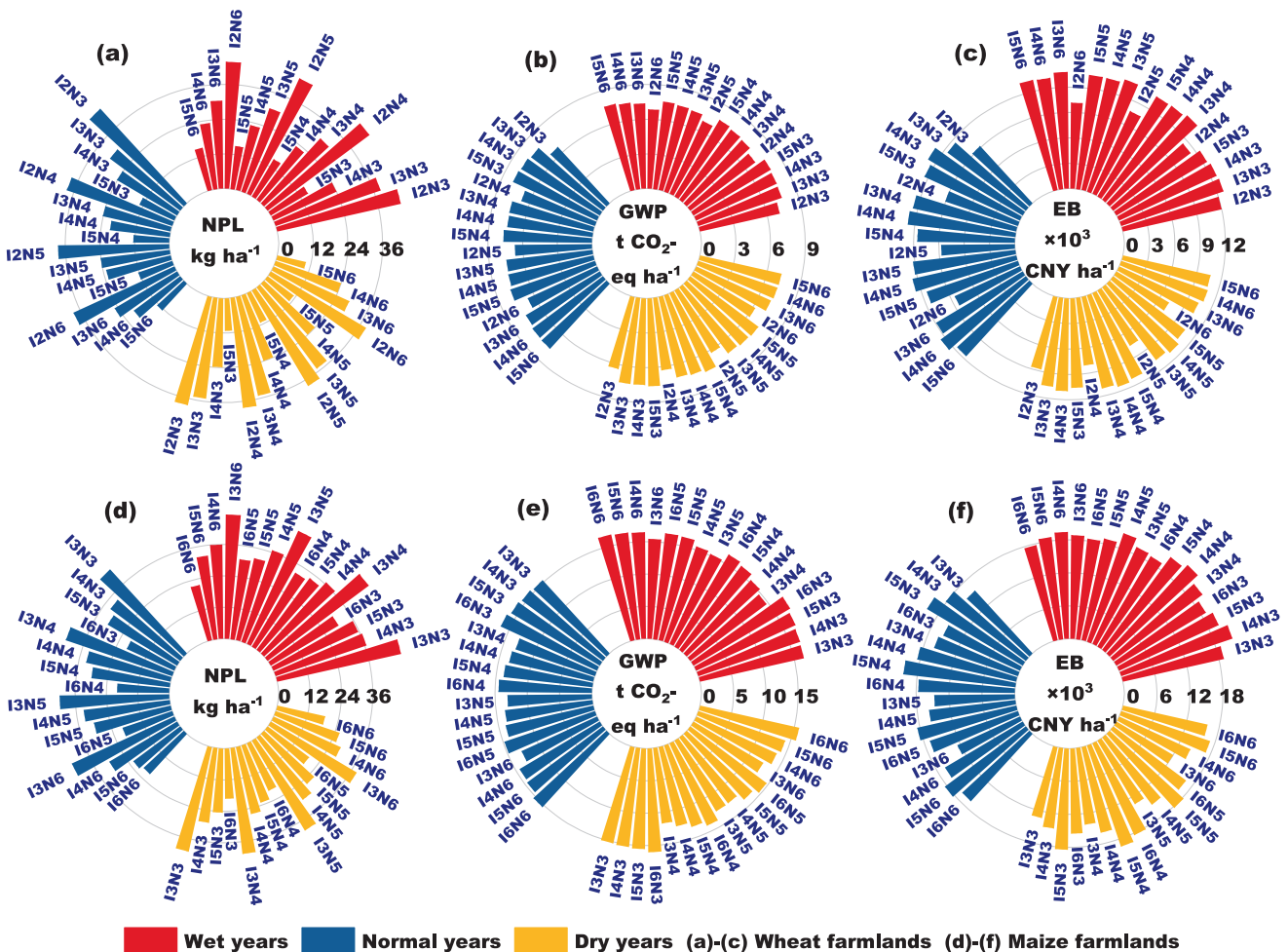


Fig. 3. NPL, GWP, and EB across irrigation and nitrogen fertilization times scenarios for wheat and maize in wet, normal, and dry years. NPL, GWP, and EB denote the nitrogen pollution load, global warming potential, and economic benefits, respectively.

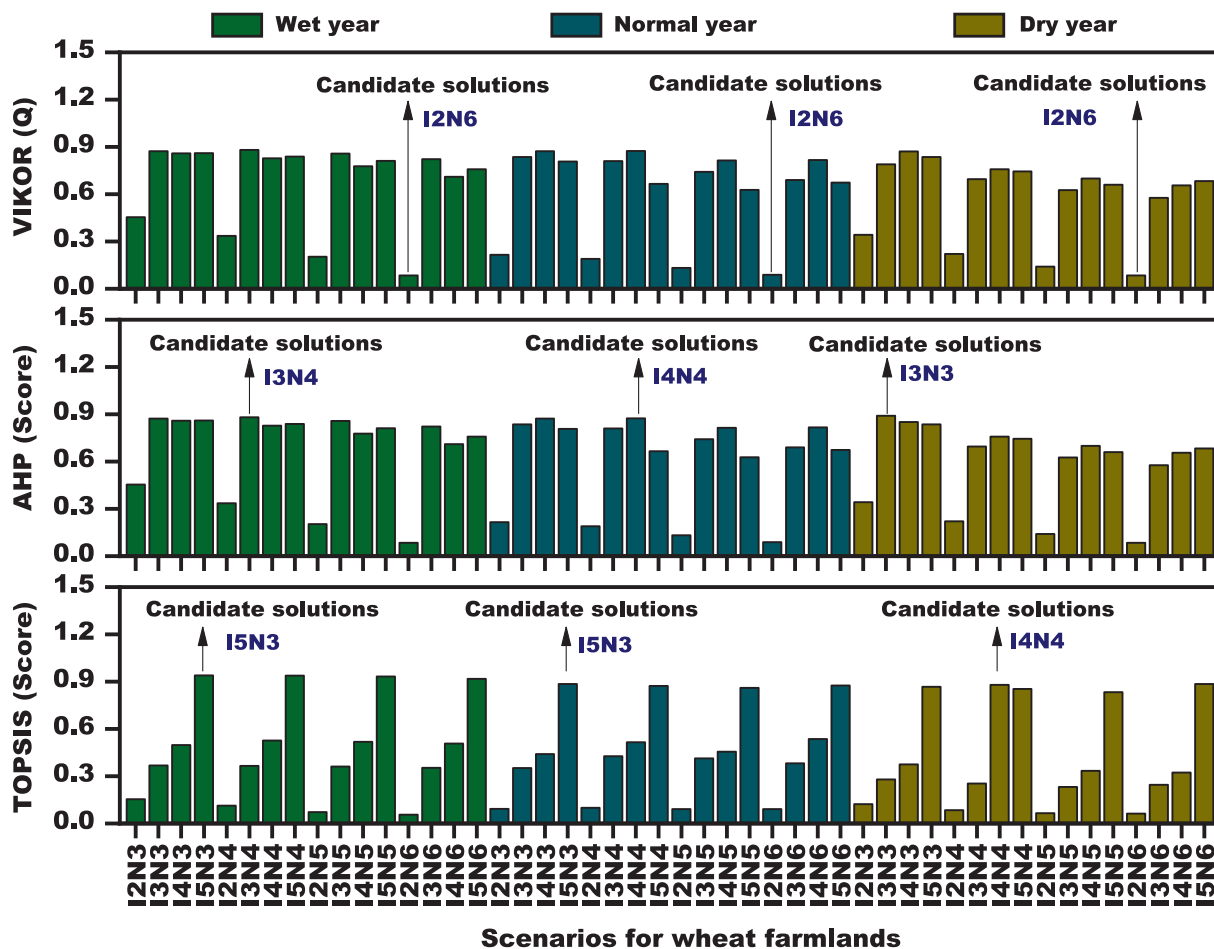


Fig. 4. First-layer decision outcomes based on MCDM methods for wheat farmlands under different irrigation and nitrogen fertilization times. Note: IxNy denotes the combination of x irrigation times and y fertilization times. For the VIKOR method, the preliminary candidate solutions were selected by ranking the benefit ratio (Q), with the lowest Q value identifying the candidate INFT. For the TOPSIS and AHP methods, the preliminary candidate solution was ranked by score, with the highest score corresponding to the candidate INFT.

selected I5N4, I5N4, and I4N4, while TOPSIS selected I6N6, I6N4, and I6N4 in wet, normal, and dry years, respectively (Fig. 5). The variation in candidate solutions among different MCDM methods suggests that relying on a single method to determine the INFT increases uncertainty and may overlook the optimal solution (Li et al., 2023a; Wu et al., 2023).

The candidate INFTs recommended by VIKOR yielded the lowest SUSI across all hydrological years and crop types (Fig. 6). This occurred because VIKOR selected a low irrigation frequency (2 times for wheat and 3 times for maize) to control the negative indicator GWP (Fig. 3). However, under a constant total irrigation amount, the low irrigation frequency resulted in a larger single irrigation depth, which increased available nitrogen losses and the risk of crop waterlogging, ultimately reducing yield and increasing NPL (Peng et al., 2019; Li et al., 2022), thus reducing SUSI (Fig. 6). The AHP method also recommended a low irrigation frequency (3 times for wheat and 4 times for maize) in dry years to mitigate GWP. In dry conditions, however, infrequent irrigation increased the risk of soil drought between adjacent irrigation events, limiting crop growth (Mon et al., 2016) and resulting in yield and EB losses, which reduced SUSI (Fig. 6). For the TOPSIS method, it focused on mitigating soil water-nitrogen pulses by increasing irrigation and fertilization times in wet and normal years to reduce NPL (Abera et al., 2018). However, the high irrigation frequency reduced the amount of water and nitrogen supplied per event during critical growth stages (tillering, jointing, and filling in wheat; V12, tasseling, and filling in maize), potentially leading to water and nutrient deficits (Shi et al., 2018; Huang et al., 2022). As a result, crop yield, IWP, and PFP_n

decreased, ultimately lowering SUSI.

In the second decision-making level, the candidate solution with the highest SUSI value was selected from those generated by VIKOR, AHP, and TOPSIS (Fig. 6) and recommended as the final INFT for each crop under different hydrological years. This demonstrates that the second decision-making layer consistently identified the solution that achieved the best overall compromise among all positive and negative indicators, thereby determining the optimal INFT. Specifically, under suitable irrigation depth (210 mm in wet years, 240 mm in normal years, and 300 mm in dry years for wheat; 270 mm, 300 mm, and 330 mm for maize) and nitrogen application rate (250 kg ha⁻¹ for both crops across hydrological years), the recommended strategies were as follows: for wheat, I3N4 (three irrigations and four nitrogen applications) in wet years, and I4N4 (four irrigations and four nitrogen applications) in normal and dry years; for maize, I5N4 (five irrigations and four nitrogen applications) in wet and normal years, and I6N4 (six irrigations and four nitrogen applications) in dry years.

4.3. Performance advantages of the decision-making framework and its driven INFT

Compared to traditional decision-making approaches that rely on externally connect individual modules (agro-hydrological model + MCDM), the two-layer intelligent decision framework developed on the COZE platform offers significant advantages in both efficiency and intelligence (Table 4). Specifically, Du et al. (2025) developed a DASSAT

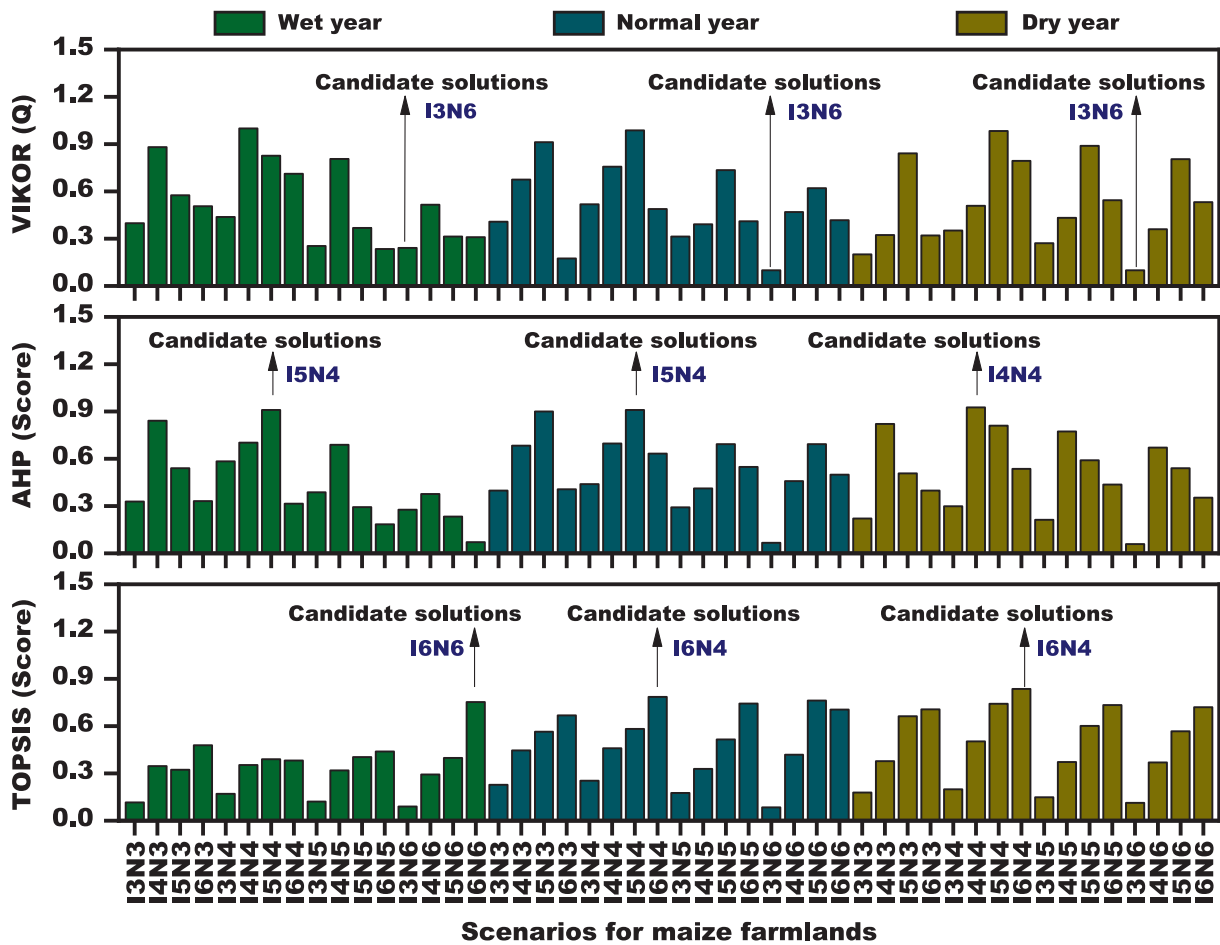


Fig. 5. First-layer decision outcomes based on MCDM methods for maize farmlands under different irrigation and nitrogen fertilization times. Note: IxNy denotes the combination of x irrigation times and y fertilization times. For the VIKOR method, the preliminary candidate solutions were selected by ranking the benefit ratio (Q), with the lowest Q value identifying the candidate INFT. For the TOPSIS and AHP methods, the preliminary candidate solution was ranked by score, with the highest score corresponding to the candidate INFT.

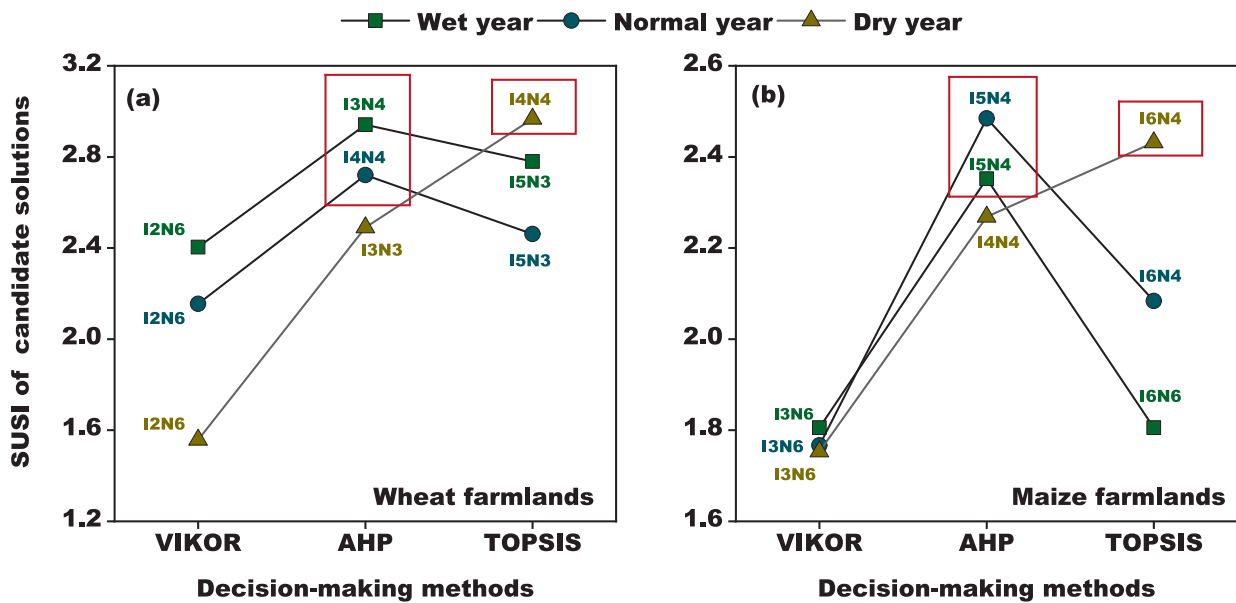


Fig. 6. Second-layer decision outcomes based on SUSI of positive and negative indicators for wheat and maize farmlands under different irrigation and nitrogen fertilization times. Note: IxNy denotes the combination of x irrigation times and y fertilization times. SUSI denotes the sustainability index. The labels enclosed in the red box denote the optimal solution finally recommended by the decision-making framework under different hydrological years.

Table 4
Performance comparison between intelligent decision-making framework and traditional methods.

Steps	Traditional method (Agro-hydrological model + MCDM) (Wu et al., 2023)	Traditional method (Agro-hydrological model + MCDM) (Li et al., 2023a)	Intelligent decision-making framework
Model operation/activation	✓	✓	✓
Model output extraction	✓	✓	×
Data format conversion	✓	✓	×
Decision indicator calculation	✓	✓	×
MCDM method execution	✓	✓	×
Time for each decision cycle	12–20 min	17–30 min	1–2 min

Note: MCDM denotes multi-criteria decision-making methods.

model combined with a machine learning-based decision-making framework for optimizing irrigation-nitrogen application schedules, while Wu et al. (2023) proposed an AHC-VIKOR framework for optimizing irrigation and nitrogen rates. Although such integrations of agro-hydrological models with machine learning or MCDM have improved decision-making efficiency compared to field

experiment-based methods, they still require considerable human intervention, such as extracting model outputs, converting data formats, calculating decision indicators, and executing MCDM procedures (Biazar et al., 2025). Moreover, the time required for these manual steps increases with the number of decision indicators (Darouich et al., 2022). For instance, in our earlier study using an AHC + VIKOR approach to balance yield, IWP, and soil salinity, one decision cycle took 12–20 min (Wu et al., 2023). When nine ecosystem service values were later added as decision indicators, the decision cycle time increased by an additional 5–10 min (Li et al., 2023a). In contrast, the framework proposed in this study can be activated simply by entering the crop type, after which the entire decision process is automatically carried out by the COZE agent on behalf of the user. By replacing extensive manual steps with an AI platform, reducing the procedure from five steps to one, the time required for a full decision cycle was shortened to just 1–2 min, which is only 6–9% of the time required by earlier methods, corresponding to an 11- to 16-fold increase in decision-making efficiency (Table 4).

The INFT optimized by the intelligent decision framework effectively enhanced agricultural productivity and economic returns while mitigating negative environmental impacts in irrigated farmland systems (Fig. 7). This improvement stems primarily from the framework’s two-layer decision mechanism: (1) MCDM methods were applied to screen candidate solutions that effectively reduce negative indicators (NPL and GWP) while maintaining high positive indicators (crop yield, IWP, PFP_n, and EB); and (2) the final solution was selected through further optimization guided by the SUSI-maximization principle. Across the three hydrological years, the optimal INFT consistently outperformed the local control (I3N3) in both farmland systems (Fig. 7). In

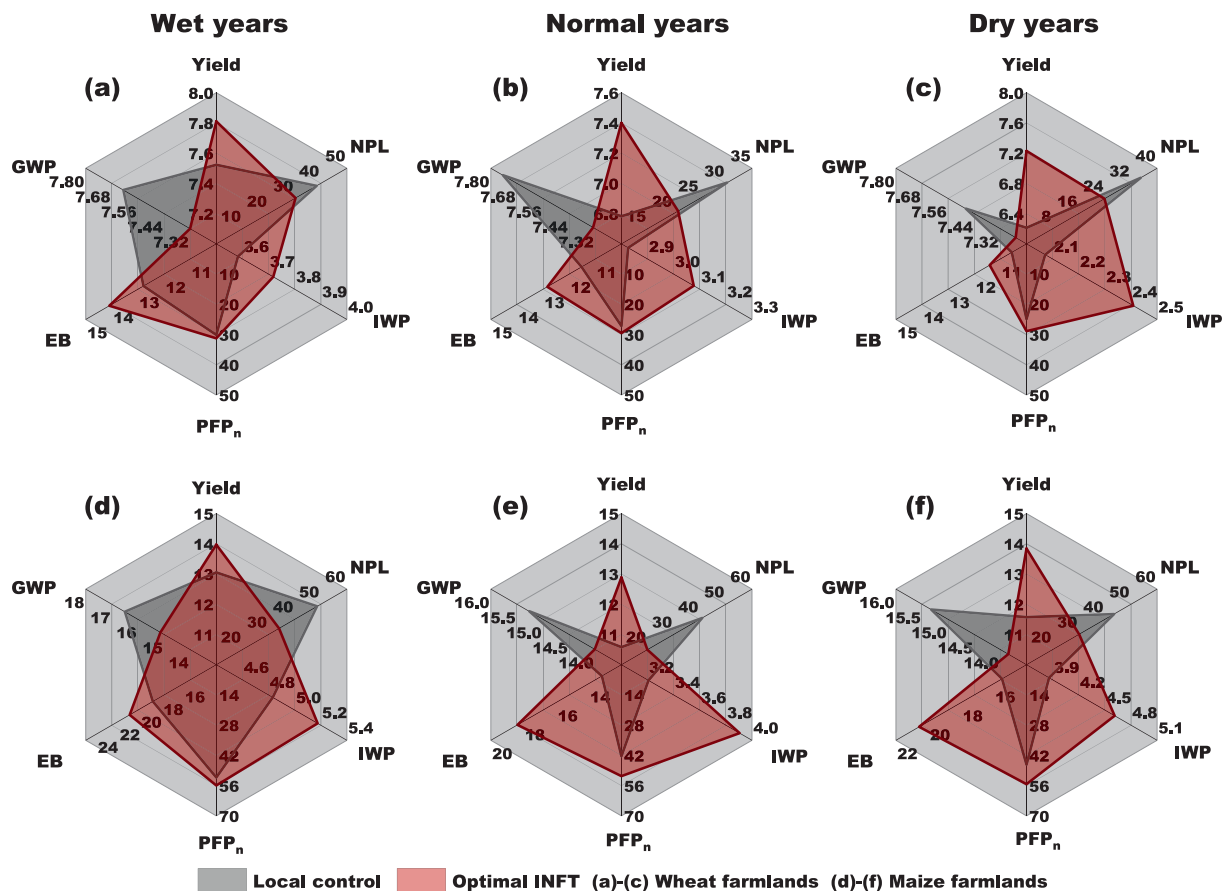


Fig. 7. Comparison of decision-making indicators between the optimal and local control scenarios. Note: INFT is the abbreviation of irrigation and nitrogen fertilization times. NPL, GWP, EB, IWP, PFP_n denote the nitrogen pollution load, global warming potential, economic benefits, irrigation water productivity, and partial factor productivity of nitrogen, respectively. The units of yield, NPL, GWP, EB, IWP, and PFP_n are t ha⁻¹, kg ha⁻¹, t CO₂-eq ha⁻¹, ×10³ CNY ha⁻¹, kg m⁻³, and kg kg⁻¹, respectively.

wheat farmlands, the optimal INFT (I3N4 for wet years and I4N4 for normal and dry years) increased crop yield, EB, IWP, and PFP_n by 3.8–16.4%, 8.0–11.4%, 3.8–16.3%, and 3.7–16.4%, respectively, and reduced NPL and GWP by 20.8–31.8% and 3.1–5.3% compared to the local control. For maize farmlands, the optimal INFT (I5N4 for wet and normal years and I6N4 for dry years) enhanced these positive indicators by 7.1–21.8%, 11.3–39.2%, 7.3–21.8%, and 7.1–21.9%, respectively, and achieved corresponding reductions of 29.9–51.2% in NPL and 8.2–9.6% in GWP relative to the local control. As a result, the optimal INFT significantly increased the SUSI by 28.5–56.1% for wheat farmlands and by 42.9–106.9% for maize farmlands relative to the local control (Fig. 8).

The underlying mechanisms can be explained by the inherent limitations of the control scenarios and the balanced optimization achieved by the two-layer framework. Under the local control, limited irrigation and fertilization events failed to replenish soil moisture and nutrients in a timely manner during critical growth stages, leading to reductions in crop yield and EB (Rubio-Asensio and Intrigliolo, 2024). Additionally, low irrigation and fertilization frequencies resulted in higher single applications of water and nitrogen. In turn, these larger individual inputs increased deep percolation and nitrate leaching (Lu et al., 2019; Li et al., 2020a). Furthermore, they triggered stronger pulses of soil CO₂ and N₂O emissions, thereby increasing GWP (Trosta et al., 2016; Tongwane and Moeletsi, 2018). In contrast, the AI-driven INFT delivered appropriate water and nitrogen supplies at critical growth stages, thus avoiding productivity losses associated with water and nitrogen

deficits or excesses (Shi et al., 2018). This approach also reduced the pollution load and climate risk linked to nitrate leaching and GHG emissions (Li et al., 2020b; Li et al., 2023b), thus increasing the SUSI of farmland systems. These results confirm that the two-layer decision framework can generate suitable irrigation and nitrogen application times that maintain high productivity while offering clear advantages in mitigating adverse environmental and climate impacts, as well as increasing sustainability in irrigated farmland systems.

4.4. Limitations and suggestions

In this study, a two-layer intelligent decision-making framework was developed by integrating an AHC model with MCDM methods (VIKOR, AHP, and TOPSIS) and introducing SUSI evaluation for decision indicators on an AI development platform. Although the framework has significantly improved decision-making efficiency and intelligence with AI support, its generalizability remains limited. This limitation stems primarily from the framework's continued reliance on agro-hydrological models as the core driver for generating the basic data. Such physically-based models typically require extensive regional data on climate, soil, crop, and groundwater to support model setup, parameter calibration, and validation, which restricts the framework's applicability in data-scarce regions (Manivasagam and Rozenstein, 2020; Wimalasiri et al., 2020).

Furthermore, although the proposed method can identify suitable INFT for target crops in irrigated farmland systems under different

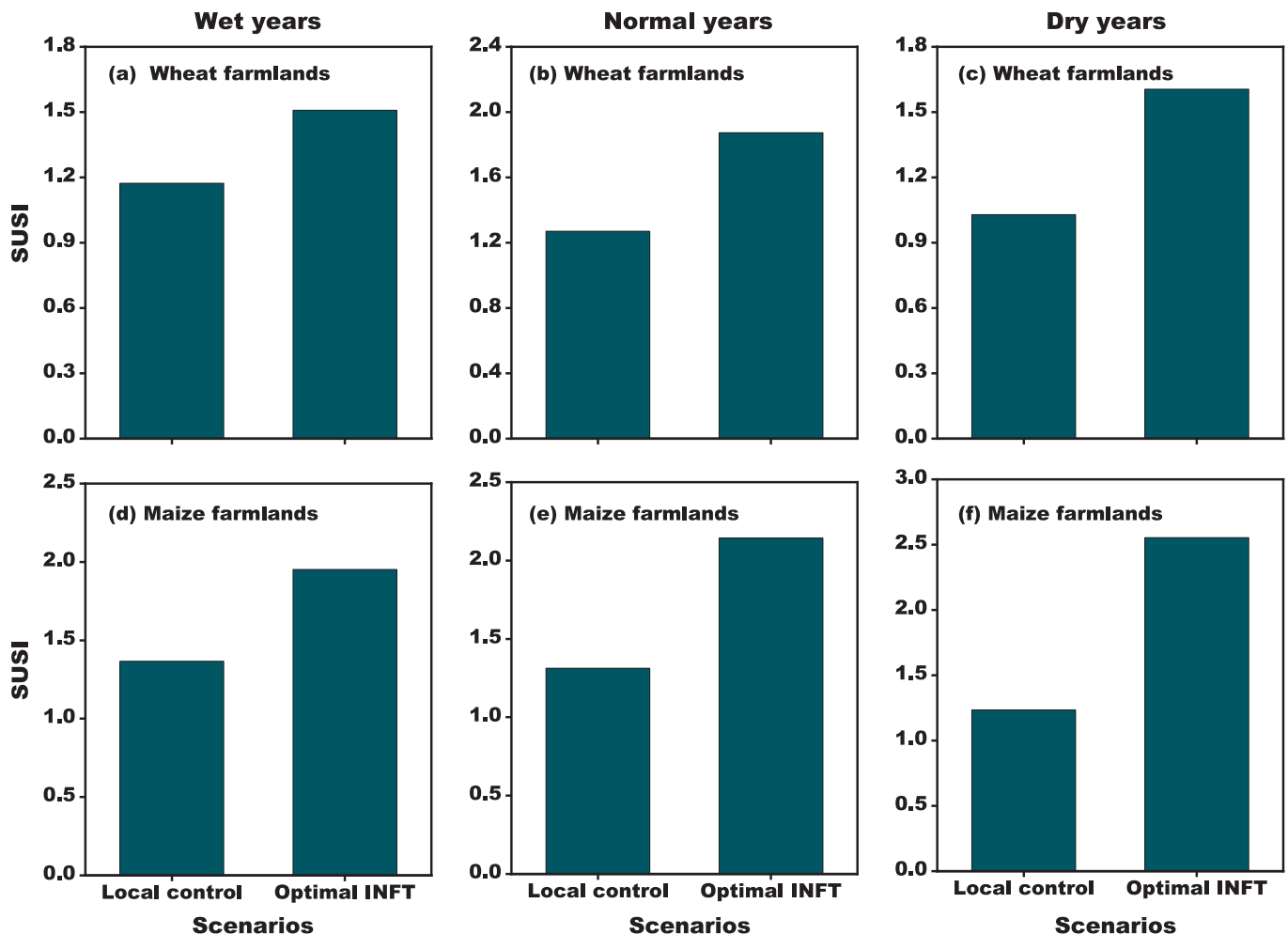


Fig. 8. Comparison of the SUSI between the optimal and local control scenarios. Note: SUSI denotes the sustainability index. INFT is the abbreviation of irrigation and nitrogen fertilization times.

hydrological years, it does not fully account for variations in precipitation patterns and soil nutrient dynamics during the crop growing season across regions and hydrological years. These factors critically influence optimal water and nitrogen management (Zeng et al., 2021; Puig et al., 2025). To address these limitations, future research should focus on: (1) exploring data-driven models, such as machine learning or deep learning, to replace or complement physically-based models, thereby reducing dependency on region-specific data and improving the transferability of the framework to data-limited regions; and (2) developing dynamic intelligent decision-making methods that incorporate real-time precipitation and soil nutrient monitoring information on AI development platform, enabling real-time recommendations for irrigation and fertilization based on actual crop needs and environmental conditions, thereby improving the spatiotemporal adaptability and decision-making precision.

5. Conclusion

Developing intelligent decision-making methods that balance productivity, economic, environmental, and climatic impacts is crucial for the efficient management of irrigation and nitrogen application. In this study, a two-layer intelligent decision-making framework was developed by integrating AHC model with MCDM methods (VIKOR, AHP, and TOPSIS) and introducing SUSI evaluation for decision indicators (yield, IWP, PFP_n, NPL, GWP, and EB) on the AI platform. Applied to wheat and maize farmlands in the HIDNC, the framework strategically determined the optimal INFT for both crops under wet, normal, and dry years by its internal MCDM-based first decision-making level and maximum SUSI-based second decision-making layer.

For wheat, three irrigations with four nitrogen applications were recommended for wet years, while four irrigations with four nitrogen applications were suggested for normal and dry years. For maize, five irrigations with four nitrogen applications were advised for wet and normal years, and six irrigations with four nitrogen applications for dry years. Compared to local control scenarios, the optimal INFT significantly improved yield, EB, IWP, and PFP_n, while reducing NPL and GWP, thereby increasing the SUSI of wheat and maize farmland systems across wet, normal, and dry years.

Moreover, the AI-based decision-making framework substantially shortened the time required for each full decision cycle compared with traditional approaches that rely on externally linked modules, achieving an 11- to 16-fold increase in decision-making efficiency. In conclusion, this study highlights how intelligent, tiered decision architectures can guide the co-optimization of irrigation and fertilization, thereby providing a feasible pathway for more autonomous and sustainable agricultural system management.

CRedit authorship contribution statement

Yue Li: Writing – review & editing, Writing – original draft, Software, Methodology, Investigation, Funding acquisition, Formal analysis, Conceptualization. **Min Hu:** Validation, Methodology, Formal analysis. **Zhijun Chen:** Software, Methodology, Conceptualization. **Yufei Han:** Resources, Data curation. **Dongyang Ren:** Validation, Supervision. **Xu Xu:** Software, Methodology, Funding acquisition. **Yunwu Xiong:** Visualization, Conceptualization. **Quanzhong Huang:** Investigation, Formal analysis. **Guanhua Huang:** Writing – review & editing, Validation, Resources, Methodology, Funding acquisition, Formal analysis, Conceptualization.

Declaration of competing interest

The authors declare that they have no known competing financial interests or personal relationships that could have appeared to influence the work reported in this paper.

Acknowledgements

This study was supported by the National Natural Science Foundation of China (grant numbers: 52220105007), the National Key R&D Program of China (grant number: 2022YFC3703702), the Postdoctoral Fellowship Program of CPSF (grant number: GZB20250568), the China Postdoctoral Science Foundation (grant number: 2025 M772478), the Key Project of Bayannur Research Institute of CAU (grant number: 2025BYNECAU004), and the Key Research Project of Science and Technology in Inner Mongolia Autonomous Region of China (grant numbers: NMKJXM202208-2, NMKJXM202301).

Appendix A. Supplementary data

Supplementary data to this article can be found online at <https://doi.org/10.1016/j.compag.2026.111721>.

Data availability

Data will be made available on request.

References

- Abera, D., Kibret, K., Beyene, S., Kebede, F., 2018. Nitrate leaching under farmers' fertilizer and irrigation water use in the central rift valley of Ethiopia. *Int. J. Phys. Soc. Sci.* 21, 1–17. <https://doi.org/10.9734/IJPSS/2018/39076>.
- Arjona, A., López, P.G., Sampé, J., Slominski, A., Villard, L., 2021. Triggerflow: trigger-based orchestration of serverless workflows. *Future Gener. Comp. Sy.* 124, 215–229. <https://doi.org/10.1016/j.future.2021.06.004>.
- Bhandari, M., Ma, Y., Men, M., Wu, M., Xue, C., Wang, Y., Li, Y., Peng, Z., 2020. Response of winter wheat yield and soil N₂O emission to nitrogen fertilizer reduction and nitrpyrin application in North China Plain. *Commun. Soil Sci. Plant Anal.* 51 (4), 554–565. <https://doi.org/10.1080/00103624.2020.1718687>.
- Biazar, S.M., Golmohammadi, G., Nedhunuri, R.R., Shaghghi, S., Mohammadi, K., 2025. Artificial intelligence in hydrology: advancements in soil, water resource management, and sustainable development. *Sustainability* 17 (5), 2250. <https://doi.org/10.3390/su17052250>.
- Darouich, H., Karfoul, R., Ramos, T.B., Moustafa, A., Pereira, L.S., 2022. Searching for sustainable-irrigation issues of clementine orchards in the Syrian Akkar Plain: Effects of irrigation method and canopy size on crop coefficients, transpiration, and water use with SIMDualKc model. *Water* 14 (13), 2052. <https://doi.org/10.3390/w14132052>.
- Diakoulaki, D., Mavrotas, G., Papayannakis, L., 1995. Determining objective weights in multiple criteria problems: the CRITIC method. *Comput. Oper. Res.* 22 (7), 763–770. [https://doi.org/10.1016/0305-0548\(94\)00059-H](https://doi.org/10.1016/0305-0548(94)00059-H).
- Dong, W., Zhang, Y., Xie, M., Hang, K., Fu, X., 2011. Efficient utilization of water and nitrogen for spring wheat high-yield in Hetiao Irrigation Region. *J. Arid. Land* 25 (6), 127–131.
- Du, J., Yang, P., Li, Y., Ren, S., Wang, Y., Li, X., Du, J., Zhang, J., He, X., 2011a. Effect of different irrigation seasons on the transfer of N in different types farmlands and the no-point pollution production. *Trans. CSAE* 27 (1), 57–64.
- Du, J., Yang, P.L., Li, Y.K., Ren, S.M., Wang, Y.Z., Li, X.Y., Lin, Y., 2011b. Nitrogen balance in the farmland system based on water balance in Hetiao Irrigation District, Inner Mongolia. *Acta Ecol. Sin.* 31 (16), 4549–4559.
- Du, R., Ma, Y., Lu, X., Xiang, Y., Zhang, F., Wang, H., Zhang, Y., Feng, X., 2025. An intelligent decision-making framework for optimizing canola irrigation-nitrogen application schedule by DSSAT model and machine learning. *Field Crops Res.* 331, 109989. <https://doi.org/10.1016/j.fcr.2025.109989>.
- He, T., Ding, W., Chen, X., Cai, Y., Zhang, Y., Xia, H., Wang, X., Zhang, J., Zhang, K., Zhang, Q., 2024. Meta-analysis shows the impacts of ecological restoration on greenhouse gas emissions. *Nat. Commun.* 15, 2668. <https://doi.org/10.1038/s41467-024-46991-5>.
- Huang, M., Wang, C., Qi, W., Zhang, Z., Xu, H., 2022. Modelling the integrated strategies of deficit irrigation, nitrogen fertilization, and biochar addition for winter wheat by AquaCrop based on a two-year field study. *Field Crops Res.* 282, 108510. <https://doi.org/10.1016/j.fcr.2022.108510>.
- IPCC, Climate Change 2021: The Physical Science Basis. Contribution of Working Group I to the Sixth Assessment Report of the Intergovernmental Panel on Climate Change (eds Masson-Delmotte, V. et al.) (Cambridge Univ. Press, 2021).
- Kamran, M., Yan, Z., Ahmad, I., Jia, Q., Ghani, M.U., Chen, X., Chang, S., Li, T., Siddique, K.H.M., Fahad, S., Hou, F., 2023. Assessment of greenhouse gases emissions, global warming potential and net ecosystem economic benefits from wheat field with reduced irrigation and nitrogen management in an arid region of China. *Agric. Ecosyst. Environ.* 341, 108197. <https://doi.org/10.1016/j.agee.2022.108197>.
- Li, C., Xiong, Y., Cui, Z., Huang, Q., Xu, X., Han, W., Huang, G., 2020a. Effect of irrigation and fertilization regimes on grain yield, water and nitrogen productivity of mulching cultivated maize (*Zea mays* L.) in the Hetiao Irrigation District of China. *Agric. Water Manag.* 232, 106065. <https://doi.org/10.1016/j.agwat.2020.106065>.

- Li, C., Xiong, Y., Huang, Q., Xu, X., Huang, G., 2020b. Impact of irrigation and fertilization regimes on greenhouse gas emissions from soil of mulching cultivated maize (*Zea mays* L.) field in the upper reaches of Yellow River, China. *J. Clean. Prod.* 259, 120873. <https://doi.org/10.1016/j.jclepro.2020.120873>.
- Li, X., Wang, P., Mu, J., Mu, D., Sun, C., Li, Z., Ren, D., Huo, Z., Xu, X., 2025. Unraveling long-term water consumption changes and agro-ecological responses to agricultural practices in arid irrigation districts of the upper Yellow River basin (2000–2021). *J. Hydrol.* 658, 133222. <https://doi.org/10.1016/j.jhydrol.2025.133222>.
- Li, Y., Huang, G., Chen, Z., Xiong, Y., Huang, Q., Xu, X., Huo, Z., 2022. Effects of irrigation and fertilization on grain yield, water and nitrogen dynamics and their use efficiency of spring wheat farmland in an arid agricultural watershed of Northwest China. *Agric Water Manag* 260, 107277. <https://doi.org/10.1016/j.agwat.2021.107277>.
- Li, Y., Xu, X., Chen, Z., Xiong, Y., Huang, Q., Huang, G., 2023a. A process simulation-based framework for resource, food, and ecology trade-off by optimizing irrigation and N management. *J. Hydrol.* 617, 129035. <https://doi.org/10.1016/j.jhydrol.2022.129035>.
- Li, Y., Xu, X., Hu, M., Chen, Z., Tan, J., Liu, L., Xiong, Y., Huang, Q., Huang, G., 2023b. Modeling water–salt–nitrogen dynamics and crop growth of saline maize farmland in Northwest China: searching for appropriate irrigation and N fertilization strategies. *Agric Water Manag* 282, 108271. <https://doi.org/10.1016/j.agwat.2023.108271>.
- López-Bellido, L., López-Bellido, R.J., Redondo, R., 2005. Nitrogen efficiency in wheat under rainfed Mediterranean conditions as affected by split nitrogen application. *Field Crops Res.* 94 (1), 86–97. <https://doi.org/10.1016/j.fcr.2004.11.004>.
- Lu, J., Bai, Z., Velthof, G.L., Wu, Z., Chadwick, D., Ma, L., 2019. Accumulation and leaching of nitrate in soils in wheat-maize production in China. *Agric Water Manag* 212, 407–415. <https://doi.org/10.1016/j.agwat.2018.08.039>.
- Lukinskiy, V., Lukinskiy, V., Bazhina, D., 2025. Refining the analytic hierarchy process: a statistical and methodological exploration of expert judgments. *Alex. Eng. J.* 125, 526–536. <https://doi.org/10.1016/j.aej.2025.04.022>.
- Manivasagam, V.S., Rozenstein, O., 2020. Practices for upscaling crop simulation models from field scale to large regions. *Comput. Electron. Agric.* 175, 105554. <https://doi.org/10.1016/j.compag.2020.105554>.
- Mon, J., Bronson, K.F., Hunsaker, D.J., Thorp, K.R., White, J.W., French, A.N., 2016. Interactive effects of nitrogen fertilization and irrigation on grain yield, canopy temperature, and nitrogen use efficiency in overhead sprinkler-irrigated durum wheat. *Field Crops Res.* 191, 54–65. <https://doi.org/10.1016/j.fcr.2016.02.011>.
- Opricovic, S., Tzeng, G., 2004. Compromise solution by MCDM methods: a comparative analysis of VIKOR and TOPSIS. *Eur. J. Oper. Res.* 156 (2), 445–455. [https://doi.org/10.1016/S0377-2217\(03\)00020-1](https://doi.org/10.1016/S0377-2217(03)00020-1).
- Peng, Z., Zhang, B., Cai, J., Wei, Z., Chen, H., Liu, Y., 2019. Optimization of spring wheat irrigation schedule in shallow groundwater area of Jiefangzha region in Hetao Irrigation District. *Water* 11 (12), 2627. <https://doi.org/10.3390/w11122627>.
- Puig, F., Garcia-Vila, M., Soriano, M.A., Rodríguez-Díaz, J.A., 2025. AquaCrop-IoT: a smart irrigation platform integrating real-time images and weather forecasting. *Comput. Electron. Agric.* 235, 110372. <https://doi.org/10.1016/j.compag.2025.110372>.
- Qi, Z., Gao, Y., Sun, C., Ramos, T.B., Mu, D., Xun, Y., Huang, G., Xu, X., 2024. Assessing water-nitrogen use, crop growth and economic benefits for maize in upper Yellow River basin: feasibility analysis for border and drip irrigation. *Agric Water Manag* 295, 108771. <https://doi.org/10.1016/j.agwat.2024.108771>.
- Rubio-Asensio, J.S., Intrigliolo, D.S., 2024. Fertigation frequency is a useful tool for nitrate management in intensive open-field agriculture. *Irrig. Sci.* 42 (2), 353–365. <https://doi.org/10.1007/s00271-023-00908-0>.
- Shalwee, Dhupper, R., Kumari, M., Gupta, A.K., Kumar, D., 2025. Implementing multi-criteria decision-making approaches to evaluate and map drought vulnerability with Geospatial Artificial Intelligence (Geo-AI) based investigations. *Discov. Appl. Sci.* 7, 1185. <https://doi.org/10.1007/s42452-025-07189-6>.
- Shi, X., Xu, Q., Hu, K., Li, S., 2018. Effect of irrigation times on nitrogen loss, water and nitrogen use efficiencies in oasis spring maize farmland. *Trans. CSAE* 34 (3), 118–126.
- Sun, Q., Zhang, Q., Yang, H., Li, B., Wu, Y., 2025. The application of a multimodal analysis system based on the COZE AI Agent in education. 2025 7th International Conference on Computer Science and Technologies in Education (CSTE), pp. 430–437. <https://ieeexplore.ieee.org/document/11092055>.
- Tongwane, M.I., Moeletsi, M.E., 2018. A review of greenhouse gas emissions from the agriculture sector in Africa. *Agr. Syst.* 166, 124–134. <https://doi.org/10.1016/j.agsy.2018.08.011>.
- Trosta, B., Prochnow, A., Meyer-Auricha, A., Drastiga, K., Baumecker, M., Ellmer, F., 2016. Effects of irrigation and nitrogen fertilization on the greenhouse gas emissions of a cropping system on a sandy soil in northeast Germany. *Eur. J. Agron.* 81, 117–128. <https://doi.org/10.1016/j.eja.2016.09.008>.
- Wimalasiri, E.M., Jahanshahi, E., Udayangani, H., Mapa, R.B., Karunaratne, A.S., Vidhanarachchi, L.P., Azam-Ali, S.N., 2020. Basic soil data requirements for process-based crop models as a basis for crop diversification. *Sustainability* 12 (18), 7781. <https://doi.org/10.3390/su12187781>.
- Wu, Z., Li, Y., Wang, R., Xu, X., Ren, D., Huang, Q., Xiong, Y., Huang, G., 2023. Evaluation of irrigation water saving and salinity control practices of maize and sunflower in the upper Yellow River basin with an agro-hydrological model based method. *Agric Water Manag* 278, 108157. <https://doi.org/10.1016/j.agwat.2023.108157>.
- Xu, X., Sun, C., Neng, F., Fu, J., Huang, G., 2018. AHC: an integrated numerical model for simulating agroecosystem processes—model description and application. *Ecol. Model.* 390, 23–39. <https://doi.org/10.1016/j.ecolmodel.2018.10.015>.
- Ye, N., Kurniawati, H., Hoerger, M., Kroese, D., Filar, J., 2025. Decision-making under uncertainty: a multidisciplinary perspective. *Ann. Oper. Res.* 355, 2775–2776. <https://doi.org/10.1007/s10479-025-06959-0>.
- Zeng, R., Yao, F., Zhang, S., Yang, S., Bai, Y., Zhang, J., Wang, J., Wang, X., 2021. Assessing the effects of precipitation and irrigation on winter wheat yield and water productivity in North China Plain. *Agric Water Manag* 256, 107063. <https://doi.org/10.1016/j.agwat.2021.107063>.
- Zhang, X., Li, Y., Chen, Z., Xu, X., Tan, J., Huang, G., 2022. Simulation of the responses of soil water, salt and maize yield to water-saving irrigation and salinity control regimes under mulched drip irrigation. *Trans. CSAE* 38 (Suppl.), 47–58.